

# Cooperative Driving in Mixed Traffic of Manned and Unmanned Vehicles based on Human Driving Behavior Understanding

Jiaxing Lu, Sanzida Hossain, Weihua Sheng, He Bai

**Abstract**—To achieve safe cooperative driving in mixed traffic of manned and unmanned vehicles, it is necessary to understand and model human drivers' driving behaviors. This paper proposed a Hidden Markov Model (HMM)-based method to analyze human driver's control and vehicle's dynamics; and then recognize the human driver's action, such as accelerating, braking, and changing lanes. With the knowledge of the human driver's actions, a probability model is used to predict the human-driven vehicle's acceleration. Such information on the driver behavior and the vehicle behavior can be used to achieve safer cooperative driving, which is realized using vehicle-to-vehicle (V2V) communication and model predictive control (MPC). The proposed method was tested and evaluated in our custom-built cooperative driving testbed. Experimental results show that the above driver action model is effective and accurate. A preliminary case study on a lane merging scenario is provided to further validate its effectiveness and capability.

## I. INTRODUCTION

With the number of autonomous vehicles (AVs) rapidly increasing [1], one of the biggest challenges is to ensure the safety of autonomous driving in the transportation system. It is expected that a transportation system with mixed traffic of both traditional human-driven vehicles and AVs will exist for a long time. Therefore, it is highly desirable to develop cooperative driving mechanisms to improve transportation safety in a heterogeneous transportation system. In the recent years, researchers have discovered a number of approaches to cooperation in a system with both humans and robots. One challenge is how to leverage human and machine intelligence, understand human driving behavior, and then coordinate the motion of human-driven vehicles and AVs. In the context of cooperative driving, understanding driving behavior has been a topic of priority in the past few decades. Given the knowledge of what the human drivers intend to do, the cooperative driving algorithm can make decisions for both the human-driven vehicles and AVs.

On the other hand, during the development of such cooperative driving algorithms, real world testing with real vehicles is inevitably expensive and dangerous. Therefore simulation is needed to accelerate and supplement the real world testing of cooperative driving. In recent years, driving

simulators have been used for vehicle algorithm development and experiment. For example, Waymo has logged data of 15 billion miles of simulated driving [2].

In this paper, we aim to tackle the problem of cooperative driving in mixed traffic of both manned and unmanned vehicles. The main contribution of this paper is as follows. First, we introduced a simulated cooperative driving testbed and an intelligent human-driven vehicle (IHV) in which a user interface is developed to assist the human driver. Second, based on the intelligent user interface, we developed a driving action recognition module to recognize different driving actions including accelerating, slowing down, braking, normally driving, changing to the left lane, and changing to the right lane. The driving models were trained using the drivers' control data (pedals and steering wheel) and vehicles' state data (velocity, acceleration, and literal position). Third, we proposed a probability model to predict the human-driven vehicle's acceleration based on different driver's actions, including speeding up, slowing down, braking, and normally driving. Data collected from the simulation testbed was used to train the model and obtain the statistical relationship between states and observations. Fourth, we conduct a preliminary case study of cooperative driving based on driver behavior understanding, in which the model output is used by a cooperative driving algorithm for lane merging involving a human-driven vehicle and an autonomous vehicle.

The rest of the paper is organized as follows. The related work is presented in Section II. The system architecture of the simulation testbed is introduced in Section III. Section IV provides the algorithms to understand driving behavior. Section V demonstrates how to incorporate the driving behavior model for optimized lane merging between an AV and an IHV. Section VI presents the experimental results. Section VII gives conclusions and future work.

## II. RELATED WORK

Cooperative driving is a vehicle control method that relies on vehicle-to-vehicle (V2V) communication to achieve coordinated vehicle movement so that the driving safety can be improved for all involved vehicles. In recent years, there are various research efforts in developing approaches and algorithms for cooperative driving. A cooperative driving strategy for connected and automated vehicles at unsignalized intersections was presented in [5], which is based on a tree representation of the solution space by combining Monte Carlo tree search and some heuristic rules to find a globally optimal passing order within a very short time.

Jiaxing Lu and Weihua Sheng (corresponding author) are with the School of Electrical and Computer Engineering, Oklahoma State University, Stillwater, OK 74078, USA, email: jiaxing.lu@okstate.edu, weihua.sheng@okstate.edu.

Sanzida Hossain and He Bai are with the School of Mechanical and Aerospace Engineering, Oklahoma State University, Stillwater, OK 74078, USA, email: he.bai@okstate.edu, sanzida.hossain@okstate.edu.

This work is supported by the National Science Foundation (NSF) Grants CISE/IIS 1910933, EHR/DUE 1928711 and CPS 2212582.

Xie *et al.* proposed two cooperative driving strategies for connected vehicles that move in heterogeneous traffic of regular vehicles and connected vehicles, in order to stabilize the traffic flow [6].

Advanced driver-assistance systems (ADAS) can assist human-drivers to improve driving safety and efficiency [7]. There has been a significant amount of research conducted to enhance the effectiveness and functionality of ADAS. Cueva *et al.*, for example, developed an ADAS using computer vision to detect drowsiness of a human driver, thereby avoiding potential traffic accidents [8]. Divakarla *et al.* proposed a cognitive ADAS for Level-4 AVs which achieved 23% energy economy increase compared to human-driven vehicles [9].

Driving behavior modeling has become an increasingly important research topic. To identify drivers' action and intent, a number of approaches were used including Support Vector Machine (SVM), Convolutional Neural Network (CNN), and Hidden Markov Model (HMM). Wang *et al.* proposed an HMM-based model to understand and recognize driver behavior based on driving data, including brake/gas pedal position and steering wheel angle [10]. Anup *et al.* investigated several algorithms for tactical driver behavior prediction using HMM, SVM, and Dynamic Bayesian Network (DBN)-based algorithm [11], respectively. Among them, HMM-based algorithms achieved the highest accuracy. Lin *et al.* developed and compared several algorithms for driver behavior identification, including Neural Network (NN), HMM, fuzzy control theory, and Gaussian Mixture Model (GMM). The author pointed out that HMM achieves higher accuracy in real-time driving behavior prediction [12]. The advantage of HMM being a probability-based model makes it easier for researchers to understand and define the relationship between different states [13]. Improving decision making in human-in-the-loop (HITL) systems is a great challenge [14]. Li *et al.* proposed a human action predictor based on sparse Bayesian learning in physical human-robot interaction (HRI) [15]. They proposed that human partner's operating force and the performance of the HRI process are the two main influence factors for the HITL system. Pang *et al.* presented an approach based on Stochastic Model Predictive Control (SMPC) to recognize human driver's action and provided two experimental scenarios to test the effectiveness and robustness of the proposed control strategy [16]. However, there lacks implementation of HITL on driving simulation and thus some potential problems are not considered, such as the delay of human reaction. HITL systems rely on a feedback loop between the human operator and the machine learning model. If delay is not considered, the machine learning model expects the human driver to react instantly, which is not realistic.

### III. THE SIMULATION TESTBED FOR COOPERATIVE DRIVING

As shown in Fig. 1, our cooperative driving testbed consists of a driving simulator and a user interface, which simulates an IHV. The driving simulator has 3 connected



Fig. 1: The cooperative driving simulation testbed.

monitors for in-vehicle view, an extra monitor for control and data display, and a Logitech G290 driving force suit (a steering wheel, pedals, and a shifter). The Carnetsoft driving simulator provides an open environment for further development [17]. It has a road map database, a script language, an interface to other devices, and user-friendly tools to configure the system.

The user interface, also called copilot, has a touch screen, a speaker, a camera, a microphone, and two embedded minicomputers. A Raspberry Pi 4B is used to implement the user interface functions, while an NVIDIA Jetson Nano is used to run a variety of machine learning tasks. The screen can display different information for the driver and also has an animated face which is capable of displaying different facial expressions.

The user interface communicates with the driving simulator to obtain the vehicle control data and status data, which are used to understand the vehicle driving behavior.

## IV. UNDERSTANDING DRIVING BEHAVIOR

### A. Recognizing human driver's action

To recognize a driver's driving action, we propose to use an HMM-based method, which consist of 6 HMMs for 6 different driving actions, as shown in Table I.

TABLE I: The driver action recognition HMM models

HMM	Corresponding Action
$H_S$	slowing down
$H_B$	braking
$H_N$	normally driving
$H_U$	accelerating
$H_L$	changing to the left lane
$H_R$	changing to the right lane

In the table, a set of 6 symbols corresponding to the 6 actions are defined and correspondingly, we have

$$\mathbf{A} = \{S, B, N, U, L, R\}$$

and a driving action  $\mathbf{a} \in \mathbf{A}$ . Each HMM consists of the parameters shown in Table II. The observations are discrete symbols converted from the raw input data using K-means clustering. For the HMMs corresponding to the longitudinal driving actions  $H_S, H_B, H_N, H_U$ , the raw input data include the vehicle's velocity, the gas pedal percentage, and the brake

pedal percentage. For the HMMs corresponding to the lateral driving actions  $H_L$  and  $H_R$ , the raw input data include the steering wheel angle, the vehicle's velocity, and the lateral position.

TABLE II: Parameters of the driver action recognition HMMs

Symbol	Meaning
$M_{\mathbf{a}}^T$	transition probability matrix
$M_{\mathbf{a}}^I$	initial probability matrix
$M_{\mathbf{a}}^E$	emission probability matrix
$S_{\mathbf{a}}$	hidden states
$O_{\mathbf{a}}$	observations

The HMMs are trained based on the Baum-Welch algorithm [18] with the data collected from the cooperative driving simulation testbed. The input sequence consists of 30 consecutive discrete data points with 33 ms interval, which are collected through a sliding window with the length of 30. In the inference stage, the K-means cluster centers for each HMM are used to convert the raw input data sequence to a formatted input sequence  $\{O_{\mathbf{a}}|\mathbf{a} \in \mathbf{A}\}$ . Then, we calculate the likelihood probabilities of  $O_{\mathbf{a}}$  fitting the corresponding HMM. After normalization, the probability distribution vector of the 6 actions  $\mathbf{P}_{\mathbf{a}}$  is obtained.

### B. Predicting human-driven vehicle's acceleration

To predict acceleration we first denote a set of 4 symbols corresponding to the 4 longitudinal driving actions  $\mathbf{A}' = \{S, B, N, U\}$ , 4 probability models for these 4 driving actions, and an action  $\mathbf{a} \in \mathbf{A}'$ . For each prediction model  $H_{\mathbf{a}}$  corresponding to action  $\mathbf{a}$ , the definition of its element is similar to the recognition model, except for the state  $S_{\mathbf{a}}$  and Observation  $O_{\mathbf{a}}$ . State  $S_{\mathbf{a}}$  represents the Cartesian product of different pedal data and velocity depending on the model it belongs to, as shown in Table III. Observation  $O_{\mathbf{a}}$  consists of a sequence of discrete acceleration  $u_i$ , converted from the continuous acceleration  $a_i$ , where  $i$  is the time index.

TABLE III: Definition of the state

Symbol	Definition
$S_{SL}$	$\{\text{Brake pedal} * \text{speed}\}$
$S_{BR}$	$\{\text{Brake pedal} * \text{speed}\}$
$S_{NM}$	$\{\text{Brake pedal} * \text{Gas pedal} * \text{speed}\}$
$S_{UP}$	$\{\text{Gas pedal} * \text{speed}\}$

To train the probability matrices, first, the initial probability matrix is set to be uniform. For transition probability matrix  $M_{\mathbf{a}}^T = \{P(S_{\mathbf{a}}^j | S_{\mathbf{a}}^i, \mathbf{a})\}$ ,

$$P(S_{\mathbf{a}}^j | S_{\mathbf{a}}^i, \mathbf{a}) = \frac{P(S_{\mathbf{a}}^i, S_{\mathbf{a}}^j, \mathbf{a})}{P(S_{\mathbf{a}}^i, \mathbf{a})}, \quad (1)$$

where  $i$  is the index of the current state and  $j$  is the index of the next state. For emission probability matrix  $M_{\mathbf{a}}^E = \{P(u_{\mathbf{a}}^t | S_{\mathbf{a}}^i, \mathbf{a})\}$ ,

$$P(u_{\mathbf{a}}^t | S_{\mathbf{a}}^i, \mathbf{a}) = \frac{P(u_{\mathbf{a}}^t, S_{\mathbf{a}}^i, \mathbf{a})}{P(S_{\mathbf{a}}^i, \mathbf{a})}, \quad (2)$$

where  $t$  is the index of the observation.

Given the action recognition probability vector  $\mathbf{P}_{\mathbf{a}}$  and the state  $S_{\mathbf{a}}^i$  corresponding to the current pedal percentage and velocity, the acceleration  $u_i$  is inferred as

$$u_i = \arg \max_{u^t} P(u^t, i), \quad (3)$$

where

$$P(u^t, i) = \sum_{\mathbf{a}} \sum_{S_{\mathbf{a}}^i} \{P(S_{\mathbf{a}}^i, \mathbf{a}) \times P(u_{\mathbf{a}}^t | S_{\mathbf{a}}^i, \mathbf{a})\}, \quad (4)$$

for each  $u^t$  in  $O_{\mathbf{a}}$ .

To calculate the acceleration in the next time step, we use the forward process to calculate the probability distribution matrix of  $S_{\mathbf{a}}^j$  based on the transition probability matrix,

$$P(S_{\mathbf{a}}^j, \mathbf{a}) = \sum_{S_{\mathbf{a}}^i} \{P(S_{\mathbf{a}}^j | S_{\mathbf{a}}^i, \mathbf{a}) \cdot P(S_{\mathbf{a}}^i, \mathbf{a})\}. \quad (5)$$

Then, the acceleration in the next time step is calculated as

$$f_j^h = u_j = \arg \max_{u^t} P(u^t, j), \quad (6)$$

which is used for modeling IHV in Section V.

## V. INCORPORATING DRIVER ACTION MODEL IN COOPERATIVE DRIVING

In this section, we discuss how the driver action model is employed to optimize coordination between an AV and an IHV. With this formulation, we improved over our past work [20] to include the stochasticity of the human state estimation. We use a lane merging example. While the motion of the AV can be directly controlled, the motion of the IHV can only be changed by the driver's inputs via advisory commands. The dynamics of the IHV is a hybrid system, which switches between two inputs: the human input and the advisory input, based on whether the driver follows and does not follow the advisory input. The human input is obtained from the behavior model in (6). Denote the event of the IHV driver following the advisory command by a binary variable  $x_k^B \in \{0, 1\}$  where the discrete-time index is given by  $k \in \mathbb{Z}_+$ . If the IHV follows the advisory command, then  $x_k^B = 1$ ; otherwise,  $x_k^B = 0$ . Then the probability of the driver following the advisory command at time step  $k$  is  $P_k^B = p[x_k^B = 1]$ . The probability of the driver not following,  $p[x_k^B = 0]$ , is  $1 - P_k^B$ .

We estimate  $P_k^B$  from the probability distribution vector of different actions in Section IV.A. It takes one time step for the driver to be alerted of the advisory command after it has been calculated. The driver takes an additional time step to respond. The probability that a driver will take the action recommended by the advisory command two time steps before is considered the probability  $P_k^B$ . We specify a lower limit  $l_i$  and an upper limit  $u_i$  for each action  $i \in [S, B, N, U]$ . Then using  $P_i$  from Section IV.A,  $P_k^B$  is calculated as

$$l_i < u_{k-2}^a < u_i \rightarrow P_k^B = P_i. \quad (7)$$

Based on the state of the vehicle, the estimated human input  $f_k^h$ , and the probability of following  $P_k^B$ , we formulate and solve a model predictive control (MPC) problem to

obtain optimal advisory commands and control inputs for the IHV and the AV, respectively.

### A. Optimization problem

The initial conditions are crucial for formulating the optimization problem. In our formulation, the initial human state is a stochastic parameter. To accommodate for this stochasticity we propose the following optimization formulation which is weighted by the probabilities of the initial state. The optimization objective here is the expectation of a cost function with respect to the distribution  $p[x_k^B]$ .

$$\min_{\theta_k} J(\theta_k) = P_k^B (\theta_k^\top Q \theta_k + c^\top \theta_k) \Big|_{x_k^B=1} + (1 - P_k^B) (\theta_k^\top Q \theta_k + c^\top \theta_k) \Big|_{x_k^B=0} \quad (8)$$

$$\text{s.t. } P_k^B \mathbf{G}_k \theta_k \Big|_{x_k^B=1} \leq P_k^B \mathbf{g}_k \Big|_{x_k^B=1} \quad (9)$$

$$(1 - P_k^B) \mathbf{G}_k \theta_k \Big|_{x_k^B=0} \leq (1 - P_k^B) \mathbf{g}_k \Big|_{x_k^B=0}. \quad (10)$$

Here,  $\theta_k \in \mathbb{R}^{n_t}$  is a vector of decision variables to optimize the system containing the control inputs to the system and binary state variables.  $Q \in \mathbb{R}^{n_t \times n_t}$  and  $c \in \mathbb{R}^{1 \times n_t}$  are the designed objective weights for the cost function.  $n_t$  is the total number of decision variables. The designed constraints are defined with  $G_k \in \mathbb{R}^{n_c \times n_t}$  and  $g_k \in \mathbb{R}^{n_c \times 1}$  where  $n_c$  is the total number of constraints. The goal is to find  $\theta_k$  at each time step  $k$  to minimize the cost function which will be designed by preference while satisfying all the constraints required to model the coordination of the IHV and the AV. We next provide some details on the constraints and the cost function in the MPC.

### B. MPC formulation

We use Discrete Hybrid Stochastic Automata (DHSA) [19] to model the motion of the IHV into the MPC problem. We consider a linear state space model for the motion of an AV

$$x_{k+1}^r = A_r x_k^r + B_r u_k^r. \quad (11)$$

The position and speed along the longitudinal axis relative to the origin are represented by  $x_k^r \in \mathbb{R}^2$ ,  $A_r$  and  $B_r$  are matrices of suitable dimensions that define the AV dynamics, and  $u^r \in \mathbb{R}$  is the input (acceleration) to the AV.

The IHV alternates between two dynamical systems:

$$\text{IHV under human control: } x_{k+1}^h = A_h x_k^h + B_h f_k^h \quad (12)$$

$$\text{IHV under advisory control: } x_{k+1}^h = A_h x_k^h + B_h u_k^a, \quad (13)$$

where  $A_h$  and  $B_h$  are matrices defining the IHV dynamics, and  $f_k^h \in \mathbb{R}$  is the human input estimated in (6), and  $u_k^a \in \mathbb{R}$  is the advisory commands for the IHV. One can deduce the solution to  $x_k$  as follows:

$$x_k^r = A_r^k x_0^r + \sum_{j=0}^{k-1} A_r^{k-j-1} B_r u_j^r, \quad (14)$$

$$x_k^h = A_h^k x_0^h + \sum_{j=0}^{k-1} A_h^{k-j-1} B_h f_j^h + \sum_{j=0}^{k-1} A_h^{k-j-1} B_h z_j^u \quad (15)$$

where  $z_k^u = x_k^B (u_k^a - f_k^h)$ , which formulates the transition of different inputs to the system based on  $x_k^B$  and is enforced as constraints in the following form:

$$z_k^u \leq (M_u - f_k^h) x_k^B, \quad z_k^u \geq (m_u - f_k^h) x_k^B \quad (16)$$

$$z_k^u \leq (u_k^a - f_k^h) - (m_u - f_k^h)(1 - x_k^B) \quad (17)$$

$$z_k^u \geq (u_k^a - f_k^h) - (M_u - f_k^h)(1 - x_k^B) \quad (18)$$

where  $M_u$  and  $m_u$  are the upper and lower limit of the input.

We use a stochastic finite state machine (sFSM) to model the stochastic transitions of the binary human state  $x_k^B$ . Let  $u_k^B \in \{0, 1\}$  denote the on/off of an advisory control at time step  $k$ . Based on the first-order Markov assumption, we prescribe the transition probability of  $x_{k+1}^B$  given  $x_k^B$  and  $u_k^B$ . Therefore, there are 8 different possibilities for transitions. Following [19], we introduce a binary variable  $w^i \in \{0, 1\}$  (an uncontrollable event) for each transition and constrain  $w^i = 1$  if and only if the  $i$ th transition occurs.

The probability of each event  $p[w_k^i]$  needs to be specified. In particular, we let  $p[w_k^2] = p_t$  which is the probability of transitioning to an advisory action. We also let  $p[w_k^6] = p_f$  which is the probability of continuously following the advisory control. We set  $p[w_k^3] = 1$ ,  $p[w_k^4] = 0$ ,  $p[w_k^7] = 1$ ,  $p[w_k^8] = 0$ . Note that  $p[w_k^i] + p[w_k^{i+1}] = 1$ ,  $i = 1, 3, 5, 7$ . The  $p_t$  and  $p_f$  may be learned from human-in-the-loop experiments. Let  $\delta_k^1 = x_k^B u_k^B$ . Then the possible transitions of the sFSM can be enforced using the following constraints:

$$w_k^1 + w_k^2 \leq u_k^B - \delta_k^1, \quad w_k^1 + w_k^2 \geq u_k^B - \delta_k^1, \quad (19)$$

$$w_k^5 + w_k^6 \leq \delta_k^1, \quad w_k^5 + w_k^6 \geq \delta_k^1, \quad (20)$$

$$-x_k^B + \delta_k^1 \leq 0, \quad -u_k^B + \delta_k^1 \leq 0, \quad (21)$$

$$u_k^B + x_k^B \leq 1 + \delta_k^1, \quad (22)$$

$$x_k^B = \sum_{j=0}^{k-1} u_j^B + C \sum_{j=0}^{k-1} w_j, \forall k \geq 1 \quad (23)$$

where  $C = [-1 \ 0 \ -1 \ 0]$ .

For collision avoidance during lane merging, the longitudinal position between the two vehicles needs to be larger than a threshold  $d_r > 0$ . To enforce that we introduce two binary variables  $b_{1,k}$  and  $b_{2,k}$  and two inequalities

$$x_{k,1}^r - x_{k,1}^h \leq -d_r + \bar{M} b_{1,k}, \quad (24)$$

$$x_{k,1}^r - x_{k,1}^h \geq d_r - \bar{M} b_{2,k} \quad (25)$$

where  $x_{k,1}$  denotes the position state and  $\bar{M}$  is a sufficiently large number.  $b_{1,k} + b_{2,k} = 1$  ensures that the safe distance  $d_r$  is satisfied at time step  $k$ . To reduce the time to reach this condition, we introduce a constraint

$$b_{1,k} + b_{2,k} \geq 1 \quad (26)$$

and minimize  $b_{1,k} + b_{2,k}$  in the objective function.

To enforce that our solution of  $w_k = [w_k^1 \ w_k^2 \ w_k^5 \ w_k^6]^\top$  realizes with at least  $\tilde{p}$  probability, we have

$$\ln \pi(w) = \sum_{k=0}^{K-1} \sum_{i=1,2,5,6} w_k^i \ln(p[w_k^i]) \geq \ln(\tilde{p}). \quad (27)$$

Let  $K$  be the length of the look-ahead window in the MPC. At time step  $k$ , the decision variables are summarized as  $\theta_k = [\mathbf{u}_k^r \ \mathbf{u}_k^a \ \mathbf{z}_k^u \ \mathbf{u}_k^B \ \mathbf{w}_k \ \delta_k^1 \ \mathbf{b}_k]$  where  $\mathbf{u}_k^r = [u_k^r, u_{k+1}^r, \dots, u_{k+K-1}^r]$  and  $\mathbf{u}_k^a, \mathbf{z}_k^u, \mathbf{u}_k^B, \mathbf{w}_k, \delta_k^1$  and  $\mathbf{b}_k$  are defined similarly to  $\mathbf{u}_k^r$ . The continuous variables are  $\mathbf{u}_k^r, \mathbf{u}_k^a$ , and  $\mathbf{z}_k^u$  while the rest are binary. For the control input that satisfies the constraints for both the  $x_k^B = 1$  and  $x_k^B = 0$  we require

$$[\mathbf{u}_k^r \ \mathbf{u}_k^a \ \mathbf{z}_k^u \ \mathbf{u}_k^B]^\top \Big|_{x_k^B=1} = [\mathbf{u}_k^r \ \mathbf{u}_k^a \ \mathbf{z}_k^u \ \mathbf{u}_k^B]^\top \Big|_{x_k^B=0}. \quad (28)$$

In the cost function, we consider five objectives: 1) Minimize the control inputs to the AV and the IHV based on their respective weights, 2) Maximize the speed of both vehicles within a speed limit for fast lane merging, 3) Minimize the number of advisory actions so that the merge can happen with reduced advisory actions, 4) Maximize the probability of the stochastic events, and 5) Minimize  $b_{1,k} + b_{2,k}$  so that  $d_r$  can be reached quickly.

The constraints from (14) to (28) are linear in  $\theta_k$  and can be written in the form of (9) and (10). With the constraints and designed objective, we apply the optimization in a receding horizon fashion and obtain the MPC solution consisting of the control inputs applied to the AV and the advisory commands conveyed to the IHV at each time step.

## VI. EXPERIMENTAL RESULTS

### A. Recognition algorithm

An experiment was conducted to test the accuracy of the proposed human-driver action recognition algorithm. The volunteers were asked to run each of the 6 driving actions 10 times. The experiment setting and results are shown in Table. IV. Totally 4197 data sequences were collected. 86.73% of them, or 3640 data sequences, were successfully recognized. As an example, Fig. 2 shows the ground truth of the gas pedal percentage, the vehicle speed during an accelerating action, and the probability change during the recognition. It can be observed as the percentage of gas pedal pressing increases, the probability of accelerating also increases.

TABLE IV: Experiment of testing the recognition algorithm

Action Name	Times	Number of		Accuracy
		Seq.	Recognized Seq.	
slowing down	10	513	405	79%
braking	10	278	216	78%
normally driving	10	1048	931	89%
accelerating	10	719	679	94%
changing left	10	846	748	88%
changing right	10	793	661	83%

### B. Prediction model

In this experiment, the probability model for predicting vehicle's acceleration was validated. Each of the 4 driving forward actions, including slowing down, accelerating, normally driving, and braking, was conducted by the volunteers 5 times. For every action instance, as soon as the action was recognized, the corresponding prediction model started

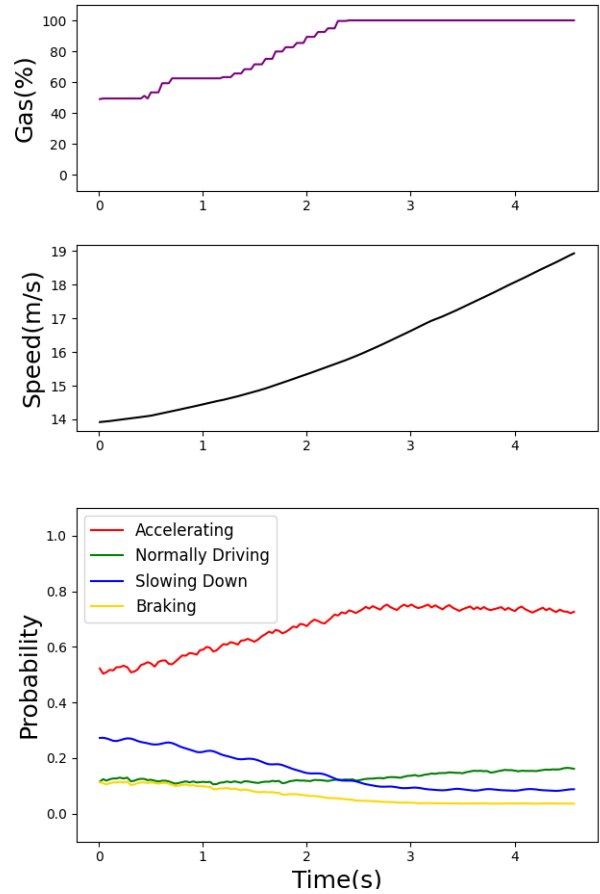


Fig. 2: Recognition of the accelerating action.

to calculate the vehicle's acceleration at the next time step. Fig. 3 and Fig. 4 show two prediction instances for accelerating and slowing down, where the red curves represent the actual accelerations during the actions and the green curves are the predicted accelerations.

### C. Optimizing lane-changing: a case study

To prove the effectiveness of the proposed driver action model, we conducted the lane merging experiment using the human driver action behavior model in the MPC optimization. The human driver action behavior model and the MPC algorithm ran on a remote computer with an Intel Core i9-11900k CPU and an NVIDIA Geforce RTX 3070 graphic card. In this experiment, the AV and the human-driven vehicle were driven alongside with the same initial speed of 15 meter/second. The AV in the left lane tried to change into the middle lane where the human-driven vehicle was in, as shown in Fig. 5. The MPC algorithm employs the action behavior model to optimize the process of establishing a safe distance before the lane merging starts.

In the first set of experiments, the volunteer followed the advice, as shown in Fig. 6a and Fig. 6b. The figure depicts the change of velocity from the starting point to when a safe distance is reached. Without the knowledge that the driver was following the advice, the system made more conservative

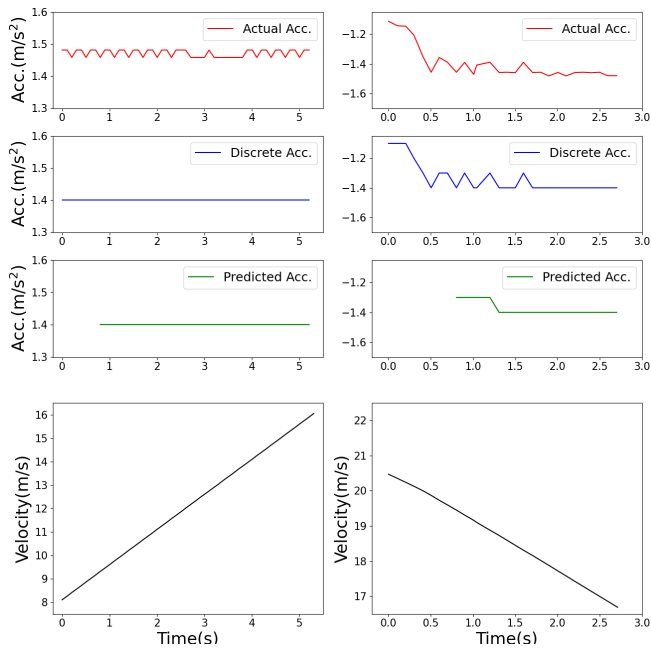


Fig. 3: Prediction of the accelerating action.

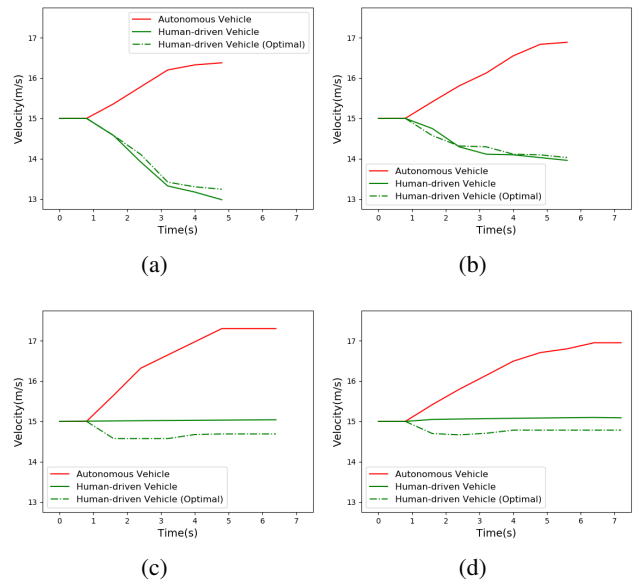


Fig. 4: Prediction of the slowing down action.

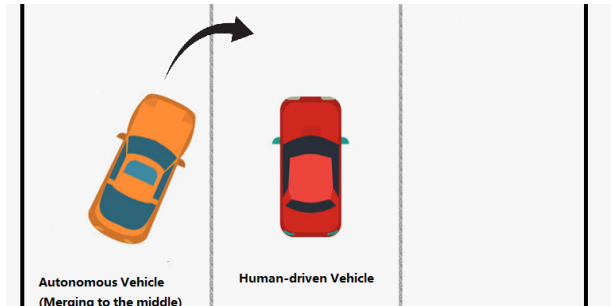


Fig. 5: Experiment scenario

advice for the IHV, resulting in a longer completion time. For another set of experiments, the volunteer did not follow the advice and kept driving normally. As shown in Fig. 6c, the system was aware that the driver was not following the advice and controlled the AV to speed up notably faster, which reduced the completion time significantly compared with the result in Fig. 6d where the system is not aware of the driver is following the advice or not.

To compare the completion time, 10 tests were conducted for each of the above four cases. Fig. 7 shows the comparison of the completion time. In the figure, the boxes demonstrate the interquartile range of the data with a line inside each box representing the median. As we can see, the behavior model significantly improved the optimization process, whether the driver was following or not.

### VII. CONCLUSIONS AND FUTURE WORK

This paper proposes the modelling of human drive behavior and investigates its use in cooperative driving for lane-changing in mixed traffic with both human-driven vehicles and autonomous vehicles. The action behavior model

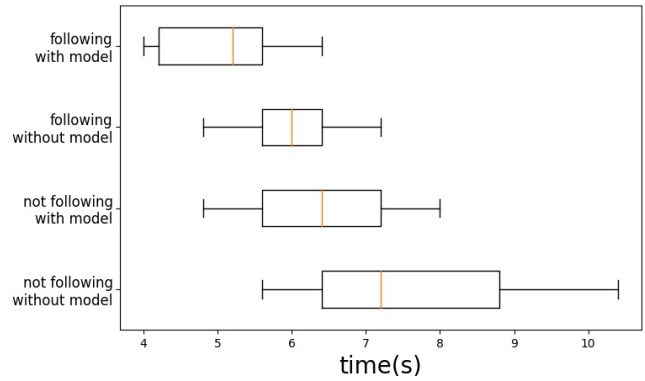


Fig. 7: Statistical results of the experiment

consists of an HMM-based model for recognizing driver's actions, and a probability model for predicting the human-driven vehicle's acceleration. We conducted experimental evaluations on a custom-built cooperative driving testbed. Experimental results show that the model helps the MPC algorithm achieve better performance in a cooperative driving scenario. Future work will consider improving the recognition and prediction model using other sensor data and investigating cooperative driving algorithms in more complicated driving scenarios.

## REFERENCES

- [1] Projected size of the global autonomous car market from 2019 to 2023. [Online]. Available: <https://www.statista.com/statistics/428692/projected-size-of-global-autonomous-vehicle-market-by-vehicle-type/>
- [2] Off road, but not offline: How simulation helps advance our Waymo Driver. [Online]. Available: <http://bit.ly/WaymoBlog>
- [3] Distracted Driving 2019. [Online]. Available: <https://crashstats.nhtsa.dot.gov/Api/Public/ViewPublication/813111>
- [4] Naumann, Maximilian Poggenhans, Fabian Lauer, Martin Stiller, Christoph. (2018). CoInCar-Sim: An Open-Source Simulation Framework for Cooperatively Interacting Automobiles. 1-6. 10.1109/IVS.2018.8500405.
- [5] H. Xu, Y. Zhang, L. Li and W. Li, "Cooperative Driving at Unsignalized Intersections Using Tree Search," in *IEEE Transactions on Intelligent Transportation Systems*, vol. 21, no. 11, pp. 4563-4571, Nov. 2020, doi: 10.1109/TITS.2019.2940641.
- [6] Dong-Fan Xie, Yong-Qi Wen, Xiao-Mei Zhao, Xin-Gang Li, Zheng-bing He (2020) Cooperative driving strategies of connected vehicles for stabilizing traffic flow, *Transportmetrica B: Transport Dynamics*, 8:1, 166-181, DOI: 10.1080/21680566.2020.1728590.
- [7] C. Wang, Q. Sun, Y. Guo, R. Fu and W. Yuan, "Improving the User Acceptability of Advanced Driver Assistance Systems Based on Different Driving Styles: A Case Study of Lane Change Warning Systems," in *IEEE Transactions on Intelligent Transportation Systems*, vol. 21, no. 10, pp. 4196-4208, Oct. 2020, doi: 10.1109/TITS.2019.2939188.
- [8] L. D. S. Cueva and J. Cordero, "Advanced Driver Assistance System for the drowsiness detection using facial landmarks," 2020 15th Iberian Conference on Information Systems and Technologies (CISTI), 2020, pp. 1-4, doi: 10.23919/CISTI49556.2020.9140893.
- [9] K. P. Divakarla, A. Emadi and S. Razavi, "A Cognitive Advanced Driver Assistance Systems Architecture for Autonomous-Capable Electrified Vehicles," in *IEEE Transactions on Transportation Electrification*, vol. 5, no. 1, pp. 48-58, March 2019, doi: 10.1109/TTE.2018.2870819.
- [10] Wang, Wenshuo Xi, Junqiang Chen, Huiyan. (2014). Modeling and Recognizing Driver Behavior Based on Driving Data: A Survey. *Mathematical Problems in Engineering*. 2014. 1-20. 10.1155/2014/245641.
- [11] A. Doshi and M. M. Trivedi, "Tactical driver behavior prediction and intent inference: A review," 2011 14th International IEEE Conference on Intelligent Transportation Systems (ITSC), 2011, pp. 1892-1897, doi: 10.1109/ITSC.2011.6083128.
- [12] Lin, Na Zong, Changfu Tomizuka, Masayoshi Song, Pan Zhang, Zexing Li, Gang. (2014). An Overview on Study of Identification of Driver Behavior Characteristics for Automotive Control. *Mathematical Problems in Engineering*. 2014. 1-15. 10.1155/2014/569109.
- [13] Q. Deng and D. Söfker, "A Review of HMM-Based Approaches of Driving Behaviors Recognition and Prediction," in *IEEE Transactions on Intelligent Vehicles*, vol. 7, no. 1, pp. 21-31, March 2022, doi: 10.1109/TIV.2021.3065933.
- [14] C. Lam, A. Y. Yang, K. Driggs-Campbell, R. Bajcsy and S. S. Sastry, "Improving human-in-the-loop decision making in multi-mode driver assistance systems using hidden mode stochastic hybrid systems," 2015 IEEE/RSJ International Conference on Intelligent Robots and Systems (IROS), 2015, pp. 5776-5783, doi: 10.1109/IROS.2015.7354197.
- [15] K. Li, R. Chen, T. Nuchkrua and S. Boonto, "Dual Loop Compliant Control Based on Human Prediction for Physical Human-Robot Interaction," 2019 58th Annual Conference of the Society of Instrument and Control Engineers of Japan (SICE), 2019, pp. 459-464, doi: 10.23919/SICE.2019.8859792.
- [16] Y. Pang, G. Zhang and H. Xia, "Autonomous Driving Traffic Control Based on Human-in-the-loop Decisions," 2021 33rd Chinese Control and Decision Conference (CCDC), 2021, pp. 1116-1121, doi: 10.1109/CCDC52312.2021.9602582.
- [17] Carnetsoft driving simulator for training and research. [Online]. Available: <https://cs-driving-simulator.com/>
- [18] L. E. Baum, A statistical estimation procedure for probabilistic functions of Markov processes, IDA-CRD Working Paper No. 131
- [19] Bemporad, Alberto, and Stefano Di Cairano. "Model-Predictive Control of Discrete Hybrid Stochastic Automata." *IEEE Transactions on Automatic Control*, vol. 56, no. 6, June 2011, pp. 1307-21. DOI.org (Crossref), <https://doi.org/10.1109/TAC.2010.2084810>.
- [20] Hossain, S., Lu, J., Bai, H. and Sheng, W. Stochastic Model Predictive Control for Coordination of Autonomous and Human-driven Vehicles. *IFAC-PapersOnLine*. 55, 142-147 (2022)